Mathematical Modelling and Analysis
Volume 28, Issue 2, 180–193, 2023
https://doi.org/10.3846/mma.2023.17583

Numerical Simulation of Fractional Power Diffusion Biosensors

Ignas Dapšys and Raimondas Čiegis

Department of Mathematical Modeling, Vilnius Gediminas Technical University
Saulėtekio al. 11, Vilnius, Lithuania
E-mail(*corresp.*): ignas.dapsys@vilniustech.lt
E-mail: rc@vgtu.lt

Received September 12, 2022; revised December 14, 2022; accepted December 15, 2022

Abstract. The main aim of this paper is to propose new mathematical models for simulation of biosensors and to construct and investigate discrete methods for the efficient solution of the obtained systems of nonlinear PDEs. The classical linear diffusion operators are substituted with nonlocal fractional powers of elliptic operators. The splitting type finite volume scheme is used as a basic template for the introduction of new mathematical models. Therefore the accuracy of the splitting scheme is investigated and compared with the symmetric Crank-Nicolson scheme. The dependence of the approximation error on the regularity of the solution is investigated. Results of computational experiments for different values of fractional parameters are presented and analysed.

Keywords: mathematical modelling, diffusion-reaction equations, fractional power of elliptic operators, finite volume schemes, splitting method, biosensors.

AMS Subject Classification: 65N08; 65N12; 65N22; 35K57.

1 Introduction

Mathematical modelling is actively used for simulation of complex biochemical processes and to optimize devices in various applications. Basic mathematical models are well described in [1], see extended lists of references presented therein.

In this paper we are studying a particular class of models which are used to simulate smart biosensors. Obtained results can be used in analysis of many similar important devices, such as smart medical bioreactors. See e.g.,

Copyright © 2023 The Author(s). Published by Vilnius Gediminas Technical University
This is an Open Access article distributed under the terms of the Creative Commons Attribution License (http://creativecommons.org/licenses/by/4.0/), which permits unrestricted use, distribution, and reproduction in any medium, provided the original author and source are credited.

[19] where reaction-diffusion equations with nonlocal boundary conditions are solved to investigate PID-controlled bioreactors, and [5, 11], where a modified nonlocal feedback controller is used to control the production of drugs in simple bioreactors.

In most models described above, linear transport processes (diffusion and convection) and nonlinear chemical reactions are investigated. In order to analyse processes with memory, mathematical models of a new type are proposed, they mostly use fractional derivative techniques to describe nonlocal transport dynamics [20, 22, 25].

There exists a similar approach when the memory effects are simulated by considering the fractional power of elliptic operators A^α. We should note that these operators can be defined in a non-unique way. In this paper we use the spectral definition (see papers [2, 3, 13, 15, 16] and more references therein). An important class of new problems is obtained when parabolic problems with fractional power elliptic operators are considered [24, 26, 27]. Non-standard effects of nonlocal diffusion processes are investigated numerically for some important applied diffusion-reaction models, see [4, 8, 21, 27].

In this paper we are interested in a generalized model of biosensors, when the classical diffusion operator is replaced by the fractional power diffusion operators. Such models present additional possibilities in solving inverse problems when the concentrations of different substrates are reconstructed from measurements of the electric current generated on the surface of the electrode.

The rest of the paper is organized in the following way. In Section 2, the mathematical problem is formulated. A standard model of biosensors is defined as a system of diffusion-reaction PDEs with appropriate initial and boundary conditions. The model is supplemented with additional information on electric current, this information is used if the inverse problem is being solved. The symmetric Crank-Nicolson finite volume scheme is constructed and investigated in Section 3. The most important part of the theoretical analysis of the symmetric finite volume scheme shows how the accuracy of the discrete solution depends on the regularity of the boundary conditions for the substrates. Some recommendations on how to preserve the classical second order accuracy in time of the Crank-Nicolson schemes are proposed.

In Section 4, a splitting type finite volume scheme is constructed, with a symmetric Crank-Nicolson type scheme as a basis. The accuracy of both schemes is compared. The presented results of computational experiments also confirm the second order accuracy in time for the splitting scheme.

In Section 5, three new mathematical models for simulation of biosensors are proposed. The main difference between classical and new mathematical models is in the description of diffusion transport – classical linear diffusion operators are substituted with nonlocal fractional power elliptic operators. The new operators are defined by applying the spectral method. The splitting type finite volume scheme is used as a basic template for the introduction of new mathematical models. Results of computational experiments for different values of fractional parameters are presented and analysed. While in the first two models the nonlocal diffusion processes are resolved by FFT algorithms, in the third (most general) model the nonlocal fractional power elliptic operators

are approximated by using the local rational operators. The BURA (Best Uniform Rational Approximation) polynomials are computed with different efficient algorithms. Some final conclusions are done in the last section.

2 Problem statement

A classical model of biosensors can be formulated as a system of diffusion-reaction PDEs [1]:

$$
\begin{aligned}
&\frac{\partial S_l}{\partial t} = D_{Se}\frac{\partial^2 S_l}{\partial x^2} - \frac{V_{max}S_l}{K_M + \sum_{k=1}^m S_k}, \quad l = 1,\dots,m, \quad 0 < x < d,\ t > 0,\\
&\frac{\partial S_l}{\partial t} = D_{Sb}\frac{\partial^2 S_l}{\partial x^2}, \quad l = 1,\dots,m, \quad d < x < d+a,\ t > 0,\\
&\frac{\partial P_l}{\partial t} = D_{Pe}\frac{\partial^2 P_l}{\partial x^2} + \frac{V_{max}S_l}{K_M + \sum_{k=1}^m S_k}, \quad l = 1,\dots,m, \quad 0 < x < d,\ t > 0, \qquad (2.1)\\
&\frac{\partial P_l}{\partial t} = D_{Pb}\frac{\partial^2 P_l}{\partial x^2}, \quad l = 1,\dots,m, \quad d < x < d+a,\ t > 0,
\end{aligned}
$$

$$
\begin{aligned}
&S_l(x,0) = 0, \quad P_l(x,0) = 0, \quad l = 1,\dots,m,\\
&D_{Se}\frac{\partial S_l}{\partial x}\big(0,t\big) = 0, \quad P_l(0,t) = 0, \quad l = 1,\dots,m,\\
&S_l(d+a,t) = s_l, \quad P_l(d+a,t) = 0, \quad l = 1,\dots,m, \qquad (2.2)
\end{aligned}
$$

where S_l are the concentrations of different substrates, P_j are products of enzyme reactions, s_l are concentrations of the substrates on the injection part of the boundary, V_{max} is the maximal enzymatic rate. We assume that each substrate has the same Michaelis-Menten constant K_M.

We note that the enzyme-catalyzed reaction is taking place in a porous enzyme-loaded microreactor ($0 \le x < d$) and no chemical reactions take place outside of it ($d < x < d+a$). The classical diffusion in space takes place in both layers, but the effective diffusion coefficients can be different in the enzyme and bulk space regions.

The classical merge conditions are specified at the boundary of two regions $x = d$ for $t > 0$ and and all components $l = 1,\dots,m$:

$$
\begin{aligned}
S_l(d-0,t) =& S_l(d+0,t), \quad D_{Se}\frac{\partial S_l}{\partial x}\big(d-0,t\big) = D_{Sb}\frac{\partial S_l}{\partial x}\big(d+0,t\big), \qquad (2.3)\\
P_l(d-0,t) =& P_l(d+0,t), \quad D_{Pe}\frac{\partial P_l}{\partial x}\big(d-0,t\big) = D_{Pb}\frac{\partial P_l}{\partial x}\big(d+0,t\big).
\end{aligned}
$$

We note that in many applications of biosensors the direct mathematical problems are not as interesting as various types of inverse problems. As an example let us assume that the concentrations of substrates on the boundary s_l, $l = 1,\dots,m$ are not known and should be reconstructed from additional measurements of the electric current generated on the surface of the electrode at $x = 0$:

$$
I(t_k) = \sum_{l=1}^m c_l D_{Pe}\frac{\partial P_l}{\partial x}\big(0,t_k\big), \quad 0 < t_1 < \ldots < t_K = T. \qquad (2.4)
$$

We also assume that the other parameters are known. Another interesting inverse problem would be the determination of the fractional power from the biosensor response, since that allows us to find an appropriate value of this parameter, based on experimental data, as well as to investigate the dependence of the fractional power on the choice of substrates, enzymes and other biosensor parameters.

The measured information is usually perturbed by noise, e.g.,

$$\widetilde{I}(t) = I(t)(1+\sigma X), \quad \text{or} \quad \widetilde{I}(t) = I(t) + \sigma X,$$

where X is a Gaussian random variable. In this paper we restrict our analysis to direct problems and are interested in new mathematical models which are based on nonlocal diffusion operators. Our aim is to obtain a wider class of mathematical models of biosensors in order to solve the formulated applied inverse problems more efficiently.

3 Finite-volume symmetric discrete scheme

The uniform spatial mesh $\bar{\omega}_h$ is defined as

$$\bar{\omega}_h = \{x_j : \ x_j = jh, \ \ j = 0, \dots, J\}, \quad x_{J_d} = d, \quad x_J = d + a.$$

To make notation more convenient, we also consider a uniform time mesh:

$$\bar{\omega}_t = \{t^n : \ t^n = n\tau, \qquad n = 0, \dots, N\}, \quad t^N = T.$$

Let $S^n_{k,j}, P^n_{k,j}$ be numerical approximations to the exact solutions $S_k(x_j, t^n)$, $P_k(x_j, t^n)$, $k = 1, \dots, m$ of the problem (2.1)–(2.3) at the grid point (x_j, t^n).

By using the finite volume method we define the following discrete diffusion operators:

$$A_{hS}S = \begin{cases} -D_{Se}\frac{2}{h}\frac{S_1 - S_0}{h}, & j = 0, \\ -\frac{1}{h}\Big(D_{S,j+\frac{1}{2}}\frac{S_{j+1}-S_j}{h} - D_{S,j-\frac{1}{2}}\frac{S_j - S_{j-1}}{h}\Big), & j = 1, \dots, J-2, \\ -\frac{1}{h}\Big(D_{Sb}\frac{-S_{J-1}}{h} - D_{Sb}\frac{S_{J-1}-S_{J-2}}{h}\Big), & j = J-1 \end{cases}$$

and

$$A_{hP}P = \begin{cases} -\frac{1}{h}\Big(D_{Pe}\frac{P_2 - P_1}{h} - D_{Pe}\frac{P_1}{h}\Big), & j = 1, \\ -\frac{1}{h}\Big(D_{P,j+\frac{1}{2}}\frac{P_{j+1}-P_j}{h} - D_{P,j-\frac{1}{2}}\frac{P_j - P_{j-1}}{h}\Big), & j = 2, \dots, J-2, \\ -\frac{1}{h}\Big(D_{Pb}\frac{-P_{J-1}}{h} - D_{Pb}\frac{P_{J-1}-P_{J-2}}{h}\Big), & j = J-1. \end{cases}$$

Here, $D_{S,j-\frac{1}{2}} = D_{Se}$, $D_{P,j-\frac{1}{2}} = D_{Pe}$ for $j = 1, \dots, J_d$ and $D_{S,j+\frac{1}{2}} = D_{Sb}$, $D_{P,j+\frac{1}{2}} = D_{Pb}$ for $j = J_d, \dots, J-1$.

It is important to note, that A_{hS} is defined for vectors satisfying the homogeneous boundary condition $S_J = 0$. This assumption is done in order to use the Fourier transform for an implementation of obtained discrete schemes.

This approach is important for the definition of nonlocal fractional powers of elliptic operators A^α, $0 < \alpha < 1$. Then the nonhomogeneous boundary conditions $S_l(d+a,t) = s_l$ should be included into the discrete scheme as specific additional source terms. These are non-local functions, due to the non-locality of fractional diffusion.

The Crank-Nicolson scheme. In this subsection we define a linearized symmetric discrete scheme. First, for a new time level $n > 0$ we apply the predictor-corrector method and solve the linearized discrete saturation equations:

$$\frac{S_l^{n-\frac{1}{2},i} - S_l^{n-1}}{0.5\tau} + A_{hS} S_l^{n-\frac{1}{2},i} = -\frac{V_{max} S_l^{n-\frac{1}{2},i-1}}{K_M + \sum_{k=1}^m S_k^{n-\frac{1}{2},i-1}} + \delta_{j,J-1} \frac{D_{Sb}}{h^2} S_{l,J}^{n-\frac{1}{2}},$$
$$l = 1, \ldots, m, \quad i = 1, 2, \tag{3.1}$$

where $S_l^{n-\frac{1}{2}} = \frac{1}{2}(S_l^n + S_l^{n-1})$ and $V_{max} = 0$, $j = J_d + 1, \ldots, J$. Iterations are defined as:

$$S_l^{n-\frac{1}{2},0} = S_l^{n-1}, \quad S_l^{n-\frac{1}{2}} = S_l^{n-\frac{1}{2},2}.$$

For each component l and fixed iteration number i the obtained linear system of equations is solved efficiently by using the standard factorization algorithm.

After solving Equations (3.1), the discrete approximations of the product P_l^n equations are formulated:

$$\frac{P_l^{n-\frac{1}{2}} - P_l^{n-1}}{0.5\tau} + A_{hP} P_l^{n-\frac{1}{2}} = \frac{V_{max} S_l^{n-\frac{1}{2}}}{K_M + \sum_{k=1}^m S_k^{n-\frac{1}{2}}}, \quad l = 1, \ldots, m, \tag{3.2}$$

where $P_l^{n-\frac{1}{2}} = \frac{1}{2}(P_l^n + P_l^{n-1})$. Again the standard factorization algorithm is used to solve these systems of linear equations.

Convergence analysis of the constructed finite volume scheme is done by using well established techniques (examples are described in [9,18]).

Theorem 1. *For a sufficiently small $\tau \le C_1$, where the constant C_1 does not depend on space mesh step h, the scheme* (3.1)–(3.2) *is unconditionally stable. If solutions of the differential problem* (2.1)–(2.2) *are sufficiently smooth functions, then the discrete solutions of the scheme* (3.1)–(3.2) *converge in the maximum norm with second order accuracy in space and time.*

Remark 1. The stability of the finite volume scheme (3.1) and the convergence rate of iterations can be improved if we use the following predictor-corrector type iterative algorithm:

$$\frac{S_l^{n-\frac{1}{2},i} - S_l^{n-1}}{0.5\tau} + A_{hS} S_l^{n-\frac{1}{2},i} = -\frac{V_{max} S_l^{n-\frac{1}{2},i}}{K_M + \sum_{k=1}^m S_k^{n-\frac{1}{2},i-1}} + \delta_{j,J-1} \frac{D_{Sb}}{h^2} S_{l,J}^{n-\frac{1}{2}}.$$

The requirement in Theorem 1 that the solution of the differential problem (2.1)–(2.2) should be sufficiently regular is nicely illustrated by considering

two different regimes of boundary conditions. For the first case, the boundary conditions (2.2) for the saturation of S_l are injected in a non-continuous way at $t = 0$:

$$S_l(d+a,t) = s_l, \quad t > 0, \quad S_l(d+a,0) = 0. \tag{3.3}$$

For the second case, the boundary conditions are introduced continuously:

$$S_l(d+a,t) = s_l \times \min(t,1), \quad t > 0. \tag{3.4}$$

In the computational experiments we consider the system with $m = 3$ components and use the following typical values of physical, chemical and geometric characteristics [1]:

$$\begin{aligned} V_{max,l} =& 5 \times 10^{-(9-l)}, \quad K_M = 1 \times 10^{-4}, \quad l = 1,2,3, \\ D_{Se} =& D_{Sb} = 4.5 \times 10^{-6}, \quad D_{Pe} = D_{Pb} = 4.5 \times 10^{-6}, \\ s_1 =& 3.88574, \quad s_2 = 11.65712, \quad s_3 = 5.25716, \\ d =& 0.02\ cm, \quad a = 0.04\ cm, \quad T = 400s. \end{aligned}$$

In order to use the same physical parameters for all mathematical models of biosensors considered in this paper, we assume that diffusion coefficients are the same in both regions. Still, for the last model, we consider a general case with different values of diffusion coefficients.

We investigated the accuracy of the discrete scheme (3.1)–(3.2) with respect to the size of time step τ. In all experiments with different solvers the space mesh sizes are fixed to $N = 999$, the test problem is solved until $T = 400$ with different time steps. The electric current $I(t_k)$ generated on the surface of the electrode at $x = 0$ was sampled every second $t_k = k$.

Table 1 gives the errors $e(\tau)$ of the discrete solution for the Crank-Nicolson scheme (3.1)–(3.2) in the maximum norm and the experimental convergence rates $\rho(\tau)$, for a sequence of decreasing time steps τ:

$$e(\tau) = \max_{k=1,\dots,400} \Big| I(t_k) - I_\tau(t_k) \Big|, \quad \rho(\tau) = \log_2 \big(e(2\tau)/e(\tau) \big),$$

where the reference solution $I(t_k)$ is computed by using a very small time step $\tau = 0.002$. Then the integration error introduced by the discrete scheme can be measured accurately.

Table 1. Errors $e_j(\tau)$ and experimental convergence rates $\rho_j(\tau)$, $j = 1,2$ for the discrete solution of the Crank-Nicolson scheme (3.1)–(3.2) for a sequence of time steps τ and two different regimes (3.3) and (3.4) of boundary conditions.

τ	$e_1(\tau)$	$\rho_1(\tau)$	$e_2(\tau)$	$\rho_2(\tau)$
0.25	4.90896	—	0.0236383	—
0.125	2.43052	1.014	0.0059078	2.000
0.0625	1.19066	1.030	0.0014752	2.001
0.03125	0.57057	1.061	0.0003670	2.006

It follows from the presented results, that the accuracy of the Crank-Nicolson discrete scheme (3.1)–(3.2) agrees well with the theoretical prediction: the accuracy is reduced to the first order for discontinuous boundary conditions (3.3) and it is restored to the optimal second order for the regularized continuous regime of boundary conditions (3.4).

4 The symmetric splitting scheme

In this section, we use the techniques proposed in [6,8], where diffusion-reaction parabolic problems with the fractional power elliptic operators are solved. We start from the symmetric finite volume scheme (3.1)–(3.2). We approximate the nonlinear reaction and linear diffusion processes separately:

$$\frac{S_{l,j}^{n-\frac{2}{3},i} - S_{l,j}^{n-1}}{\frac{1}{2}\tau} = -\frac{V_{max}\frac{1}{2}\big(S_{l,j}^{n-\frac{2}{3},i-1} + S_{l,j}^{n-1}\big)}{K_M + \sum_{k=1}^{m}\frac{1}{2}\big(S_{k,j}^{n-\frac{2}{3},i-1} + S_{k,j}^{n-1}\big)}, \tag{4.1}$$

$$l = 1,\dots,m,\quad i = 1,2,\quad j = 0,\dots,J_d,$$

$$S_{l,j}^{n-\frac{2}{3},0} = S_{l,j}^{n-1},\quad S_{l,j}^{n-\frac{2}{3}} = S_{l,j}^{n-\frac{2}{3},2},$$

$$\frac{P_{l,j}^{n-\frac{2}{3}} - P_{l,j}^{n-1}}{\frac{1}{2}\tau} = \frac{V_{max}\frac{1}{2}\big(S_{l,j}^{n-\frac{2}{3}} + S_{l,j}^{n-1}\big)}{K_M + \sum_{k=1}^{m}\frac{1}{2}\big(S_{k,j}^{n-\frac{2}{3}} + S_{k,j}^{n-1}\big)}, \tag{4.2}$$

$$\frac{S_l^{n-\frac{1}{3}} - S_l^{n-\frac{2}{3}}}{\tau} + A_{hS}\frac{S_l^{n-\frac{1}{3}} + S_l^{n-\frac{2}{3}}}{2} = \delta_{j,J-1}\frac{D_{Sb}}{h^2}\frac{S_{l,J}^{n-\frac{1}{3}} + S_{l,J}^{n-\frac{2}{3}}}{2},$$

$$l = 1,\dots,m, \tag{4.3}$$

$$\frac{P_l^{n-\frac{1}{3}} - P_l^{n-\frac{2}{3}}}{\tau} + A_{hP}\frac{P_l^{n-\frac{1}{3}} + P_l^{n-\frac{2}{3}}}{2} = 0,\quad l = 1,\dots,m, \tag{4.4}$$

$$\frac{S_{l,j}^{n,i} - S_{l,j}^{n-\frac{1}{3}}}{\frac{1}{2}\tau} = -\frac{V_{max}\frac{1}{2}\big(S_{l,j}^{n,i-1} + S_{l,j}^{n-\frac{1}{3}}\big)}{K_M + \sum_{k=1}^{m}\frac{1}{2}\big(S_{k,j}^{n,i-1} + S_{k,j}^{n-\frac{1}{3}}\big)}, \tag{4.5}$$

$$l = 1,\dots,m,\quad i = 1,2,\ S_{l,j}^{n,0} = S_{l,j}^{n-\frac{1}{3}},\quad j = 0,\dots,J_d,$$

$$\frac{P_{l,j}^{n} - P_{l,j}^{n-\frac{1}{3}}}{\frac{1}{2}\tau} = \frac{V_{max}\frac{1}{2}\big(S_{l,j}^{n} + S_{l,j}^{n-\frac{1}{3}}\big)}{K_M + \sum_{k=1}^{m}\frac{1}{2}\big(S_{k,j}^{n} + S_{k,j}^{n-\frac{1}{3}}\big)}, l = 1,\dots,m,\quad j = 0,\dots,J_d, \tag{4.6}$$

The convergence analysis of the constructed splitting finite volume scheme can be done by using well established techniques. The main difference in comparison to the analysis of symmetric Crank-Nicolson scheme is that the splitting error should be taken into account for the obtained error estimates (see [10,18]).

Theorem 2. *For a sufficiently small $\tau \le C_2$, where the constant C_2 does not depend on space mesh step h, the scheme* (4.1)–(4.6) *is unconditionally stable. If solutions of the differential problem* (2.1)–(2.2) *are sufficiently smooth functions, then the discrete solutions of the scheme* (4.1)–(4.6) *converge in the maximum norm with second order accuracy in space and time.*

The requirement that the solution of the differential problem must be sufficiently regular is again nicely seen in experimental results by considering two different regimes of boundary conditions.

Table 2 gives the errors $e_2(\tau)$ of the discrete solution for the splitting scheme (4.1)–(4.6) and the experimental convergence rates $\rho_2(\tau)$, for a sequence of decreasing time steps τ. Here we consider only the regularized continuous regime of boundary conditions.

Table 2. Errors $e_2(\tau)$ and experimental convergence rates $\rho_2(\tau)$ for the discrete solution of the splitting scheme (4.1)–(4.6) for a sequence of time steps τ and continuous regime of the boundary conditions.

τ	$e_2(\tau)$	$\rho_2(\tau)$
0.25	4.3350	—
0.125	1.0838	1.9999
0.0625	0.2709	2.0001
0.03125	0.067735	1.9998

It follows from the presented results, that the accuracy of the splitting discrete scheme agrees with the theoretical prediction, it is equal to the second order for the regularized continuous regime of boundary conditions.

Still the global error of the solution of the splitting scheme (4.1)–(4.6) is larger than the integration error of the Crank-Nicolson type discrete scheme (3.1)–(3.2).

5 Fractional powers of elliptic operators

In this section, we assume that the diffusion coefficients are constant in both regions of the domain:

$$D_{Se} = D_{Sb} = D_S, \quad D_{Pe} = D_{Pb} = D_P.$$

Let us define the following diffusion operators:

$$\mathcal{A}_{hS} S = \begin{cases} -\frac{2}{h}\frac{S_1 - S_0}{h}, & j = 0, \\ -\frac{1}{h}\left(\frac{S_{j+1}-S_j}{h} - \frac{S_j - S_{j-1}}{h}\right), & j = 1, \dots, J-2, \\ -\frac{1}{h}\left(\frac{-S_{J-1}}{h} - \frac{S_{J-1}-S_{J-2}}{h}\right), & j = J-1 \end{cases}$$

and

$$\mathcal{A}_{hP} P = \begin{cases} -\frac{1}{h}\left(\frac{P_2 - P_1}{h} - \frac{P_1}{h}\right), & j = 1, \\ -\frac{1}{h}\left(\frac{P_{j+1}-P_j}{h} - \frac{P_j - P_{j-1}}{h}\right), & j = 2, \dots, J-2, \\ -\frac{1}{h}\left(\frac{-P_{J-1}}{h} - \frac{P_{J-1}-P_{J-2}}{h}\right), & j = J-1. \end{cases}$$

Next, we define two inner products for discrete functions S and P, they take into account the appropriate homogeneous boundary conditions:

$$(S_l, S_k)_S = S_{l,0}S_{k,0}\frac{h}{2} + \sum_{j=1}^{J-1} S_{l,j}S_{k,j}h, \quad (P_l, P_k)_P = \sum_{j=1}^{J-1} P_{l,j}P_{k,j}h.$$

It is easy to see that discrete operators $\mathcal{A}_{hS}$ and $\mathcal{A}_{hP}$ are self-adjoint and positive definite. Thus they admit two systems of eigenfunctions Φ_{Sj} and Φ_{Pj} with corresponding eigenvalues $\lambda_{Sj} > 0$ and $\lambda_{Pj} > 0$, such that:

$$\begin{aligned} \mathcal{A}_{hS}\Phi_{Sj} &= \lambda_{Sj}\Phi_{Sj}, \quad j = 0, \dots, J-1, \\ \mathcal{A}_{hP}\Phi_{Pj} &= \lambda_{Pj}\Phi_{Pj}, \quad j = 1, \dots, J-1. \end{aligned}$$

Then the fractional powers of operators $\mathcal{A}_{hS}$ and $\mathcal{A}_{hP}$ are defined as:

$$\mathcal{A}_{hS}^{\alpha}S = \sum_{j=0}^{J-1} \lambda_{Sj}^{\alpha}(S, \Phi_{Sj})_S\Phi_{Sj}, \quad \mathcal{A}_{hP}^{\alpha}P = \sum_{j=1}^{J-1} \lambda_{Pj}^{\alpha}(P, \Phi_{Pj})_P\Phi_{Pj},$$

where the fractional power parameter $0 < \alpha < 1$.

It is easy to see that $\mathcal{A}_{hS}^{\alpha}$, $\mathcal{A}_{hP}^{\alpha}$ are also self-adjoint and positive definite operators.

We define the first modified biosensor model, where instead of linear diffusion equations (4.3), (4.4), nonlocal diffusion equations are used:

$$\begin{aligned} &\frac{S_l^{n-\frac{1}{3}} - S_l^{n-\frac{2}{3}}}{\tau} + D_S\mathcal{A}_{hS}^{\alpha}\frac{S_l^{n-\frac{1}{3}} + S_l^{n-\frac{2}{3}}}{2} = \frac{D_S}{h^2}\mathcal{A}_{hS}^{(\alpha-1)}\delta_{j,J-1}\frac{S_{l,J}^{n-\frac{1}{3}} + S_{l,J}^{n-\frac{2}{3}}}{2}, \\ &l = 1, \dots, m, \\ &\frac{P_l^{n-\frac{1}{3}} - P_l^{n-\frac{2}{3}}}{\tau} + D_P\mathcal{A}_{hP}^{\alpha}\frac{P_l^{n-\frac{1}{3}} + P_l^{n-\frac{2}{3}}}{2} = 0, \quad l = 1, \dots, m. \end{aligned}$$

The obtained linear equations can be solved efficiently by using the FFT algorithm. For completeness of the model we present the eigenvectors Φ_{Sj} and Φ_{Pj} and corresponding eigenvalues λ_{Sj}, λ_{Pj} explicitly:

$$\begin{aligned} &\Phi_{Sk,j} = \cos\left(\pi\frac{(j-0.5)k}{J}\right), \quad \lambda_{Sj} = \frac{4}{h^2}\sin^2\left(\frac{\pi}{2}\frac{(j-0.5)}{J}\right), \quad k, j = 1, \dots, J, \\ &\Phi_{Pk,j} = \sin\left(\pi\frac{kj}{J}\right), \quad \lambda_{Pj} = \frac{4}{h^2}\sin^2\left(\frac{\pi}{2}\frac{j}{J}\right), \quad k, j = 1, \dots, J-1. \end{aligned}$$

Computational experiments. Our main aim is to investigate how the solution of the mathematical model of biosensors depends on the fractional power parameter α. In Figure 1, the graphs of the electric current (2.4) function are presented for three different values of α.

It follows from the presented results that the value of the fractional parameter has a strong influence on the dynamics of the electric current. The current reaches the stationary value later and these absolute values are larger for decreased values of parameters α.

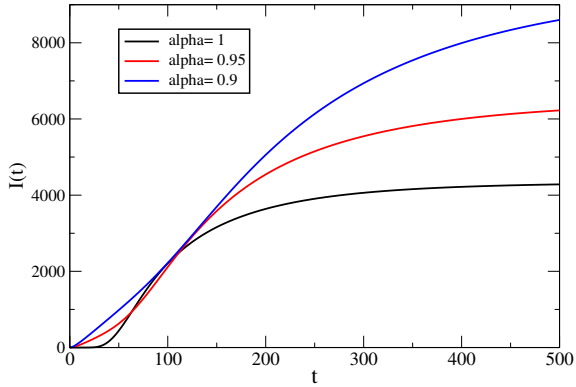

Figure 1. The dynamics of the electric current function $I(t)$ for three fractional orders: a) $\alpha = 1$, b) $\alpha = 0.95$, c) $\alpha = 0.9$.

The second generalized model of biosensors is based on a direct usage of the operators A_{hS} and A_{hP}:

$$\frac{S_l^{n-\frac{1}{3}} - S_l^{n-\frac{2}{3}}}{\tau} + A_{hS}^{\alpha} \frac{S_l^{n-\frac{1}{3}} + S_l^{n-\frac{2}{3}}}{2} = A_{hS}^{(\alpha-1)} \frac{D_{Sb}}{h^2} \delta_{j,J-1} \frac{S_{l,J}^{n-\frac{1}{3}} + S_{l,J}^{n-\frac{2}{3}}}{2},$$
$$l = 1, \ldots, m, \tag{5.1}$$

$$\frac{P_l^{n-\frac{1}{3}} - P_l^{n-\frac{2}{3}}}{\tau} + A_{hP}^{\alpha} \frac{P_l^{n-\frac{1}{3}} + P_l^{n-\frac{2}{3}}}{2} = 0, \quad l = 1, \ldots, m. \tag{5.2}$$

In the case of constant diffusion coefficients the system of eigenvectors remains the same and only trivial changes in computation of corresponding eigenvalues should be done. The FFT algorithm is used to solve the Equations (5.1) and (5.2).

Computational experiments. Again our aim is to investigate how the solution of the biosensor mathematical model depends on the fractional power parameter α. In Figure 2, the graphs of the electric current (2.4) function are presented for three different values of α.

It follows from the presented results that the dynamics of the electric current has a different dependence on the value of the fractional parameter. The current reaches the stationary value faster but these absolute values are smaller for decreased values of parameters α.

The third mathematical model of biosensors is tailored to a general case of non-constant diffusion coefficients. In order to solve it we apply the algorithm which gives an approximation of the solutions of the nonlocal diffusion equations (5.1)–(5.2). This algorithm uses the method which is proposed in [6, 7]. It is based on rational approximations of nonlocal operators. As an example we analyse the Equation (5.2) for a product function. Let us introduce a new function:

$$\widetilde{P}_l^{n-\frac{1}{2}} = \frac{1}{2}\big(P_l^{n-\frac{1}{3}} + P_l^{n-\frac{2}{3}}\big).$$

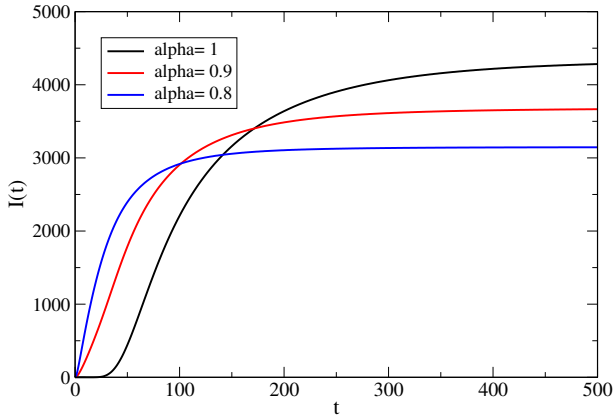

Figure 2. The dynamics of the electric current function $I(t)$ for three fractional orders: a) $\alpha = 1$, b) $\alpha = 0.9$, c) $\alpha = 0.8$.

Then (5.2) can be rewritten in the following modified form:

$$\widetilde{P}_l^{n-\frac{1}{2}} = (I_h + 0.5\tau A_h^\alpha)^{-1} P_l^{n-\frac{2}{3}}. \tag{5.3}$$

Next we approximate the nonlocal operator $(I_h + 0.5\tau A_h^\alpha)^{-1}$, by a local rational operator:

$$(I_h + 0.5\tau A_h^\alpha)^{-1} \approx r_M(A_h),$$

where a function $r_M(z)$ is defined as:

$$r_M(\lambda) = p_M(\lambda)/q_M(\lambda)$$

with polynomials p_M and q_M of the same degree M. As a practical implementation of this approach a few efficient methods can be used. Most of them are variants of the well-known BURA (Best Uniform Rational Approximation) method (for a detailed description and theoretical analysis of these algorithms see [12, 14, 17]). There, r_M is a best rational approximation of the function: $f(\lambda) = 1/(1 + 0.5\tau\lambda^\alpha)$, $\lambda \in [\lambda_{min}, \lambda_{max}]$.

A very accurate approximation $\widetilde{r}_M$ of the required rational function r_M can be computed by applying the BRASIL algorithm, which is based on the barycentric rational formula [17]. In computational experiments done in [7] we used a free and open-source implementation of this algorithm in Python. We note that there are more implementations for the construction of BURA approximations, see e.g. [23].

The constructed rational function r_M can be written in a partial fraction decomposition form [8]:

$$\widetilde{r}_M(\lambda) = c_0 + \sum_{j=1}^{M} \frac{c_j}{\lambda - d_j}.$$

Then the following scheme is constructed to compute the approximation of the solution of Equation (5.3):

$$\widetilde{P}_l^{n-\frac{1}{2}} = \Big(c_0 I + \sum_{j=1}^{M} c_j \big(A_{hP} - d_j I\big)^{-1}\Big) P_l^{n-\frac{2}{3}}.$$

Its implementation is efficient if all coefficients d_j are non-positive. The results of stability and accuracy analysis obtained in [7] confirm that this requirement is satisfied for the given class of equations when the BRASIL algorithm is used to define rational approximations.

As an additional bonus of this algorithm we note that all $(M+1)$ subproblems are independent and can be solved in parallel.

6 Conclusions

A new class of mathematical models of biosensors is proposed. The fractional powers of elliptic operators are used to simulate the nonlocal diffusion process. This generalization also covers the classical mathematical models, it is sufficient to use a special value of the fractional parameter $\alpha = 1$.

The new models are introduced for systems of parabolic problems by considering discrete approximations of the classical models of biosensors. As a basic template we use the splitting scheme since this approach is quite flexible and allows us to take into account non-homogeneous boundary conditions. This point is important when the spectral definition of fractional powers of elliptic operators is applied.

The accuracy of the proposed splitting schemes is investigated for non-regular solutions of the differential mathematical models. The obtained theoretical results allow us to formulate recommendations on how to inject boundary conditions in simulations of real biosensors.

Results of computational experiments are presented and analysed when different values of fractional power parameters are used for new mathematical models of biosensors.

References

[1] R. Baronas, F. Ivanauskas and J. Kulys. *Mathematical Modeling of Biosensors, Second Edition.* Springer, 2021. https://doi.org/10.1007/978-3-030-65505-1.

[2] A. Bonito, J.P. Borthagaray, R.H. Nochetto, E. Otárola and A.J. Salgado. Numerical methods for fractional diffusion. *Computing and Visualization in Science*, **19**(5):19–46, 12 2018. https://doi.org/10.1007/s00791-018-0289-y.

[3] A. Bonito and J.E. Pasciak. Numerical approximation of fractional powers of elliptic operators. *Mathematics of Computation*, **84**(295):2083–2110, 3 2015. https://doi.org/10.1090/s0025-5718-2015-02937-8.

[4] A. Bueno-Orovio, D. Kay and K. Burrage. Fourier spectral methods for fractional-in-space reaction-diffusion equations. *BIT Numerical Mathematics*, **54**(4):937–954, 12 2014. https://doi.org/10.1007/s10543-014-0484-2.

[5] R. Čiegis and Rem. Čiegis. Numerical algorithms for solving the optimal control problem of simple bioreactors. *Nonlinear Analysis: Modelling and Control*, **24**(4):626–638, 6 2019. https://doi.org/10.15388/NA.2019.4.8.

[6] R. Čiegis, Rem. Čiegis and I. Dapšys. A comparison of discrete schemes for numerical solution of parabolic problems with fractional power elliptic operators. *Mathematics*, **9**(12), 6 2021. https://doi.org/10.3390/math9121344.

[7] R. Čiegis and I. Dapšys. On a Framework for the Stability and Convergence Analysis of Discrete Schemes for Nonstationary Nonlocal Problems of Parabolic Type. *Mathematics*, **10**(13):2155, 6 2022. https://doi.org/10.3390/math10132155.

[8] R. Čiegis, I. Dapšys and Rem. Čiegis. A Comparison of Parallel Algorithms for Numerical Solution of Parabolic Problems with Fractional Power Elliptic Operators. *Axioms*, **11**(3):98, 2 2022. https://doi.org/10.3390/axioms11030098.

[9] R. Čiegis, P. Katauskis and V. Skakauskas. The robust finite-volume schemes for modeling nonclassical surface reactions. *Nonlinear Analysis: Modelling and Control*, **23**(2):234–250, 4 2018. https://doi.org/10.15388/NA.2018.2.6.

[10] R. Čiegis, G. Panasenko, K. Pileckas and V. Šumskas. ADI scheme for partially dimension reduced heat conduction models. *Computers & Mathematics with Applications*, **80**(5):1275–1286, 2020. https://doi.org/10.1016/j.camwa.2020.06.012.

[11] R. Čiegis, O. Suboč and Rem. Čiegis. Numerical simulation of nonlocal delayed feedback controller for simple bioreactors. *Informatica*, **29**(2):233–249, 1 2018. https://doi.org/10.15388/Informatica.2018.165.

[12] S. Harizanov, N. Kosturski, I. Lirkov, S. Margenov and Y. Vutov. Reduced multiplicative (BURA-MR) and additive (BURA-AR) best uniform rational approximation methods and algorithms for fractional elliptic equations. *Fractal and Fractional*, **5**(3):61, 6 2021. https://doi.org/10.3390/fractalfract5030061.

[13] S. Harizanov, R. Lazarov, S. Margenov, P. Marinov and J. Pasciak. Analysis of numerical methods for spectral fractional elliptic equations based on the best uniform rational approximation. *Journal of Computational Physics*, **408**:109285, 5 2020. https://doi.org/10.1016/j.jcp.2020.109285.

[14] S. Harizanov, R. Lazarov, S. Margenov, P. Marinov and Y. Vutov. Optimal solvers for linear systems with fractional powers of sparse SPD matrices. *Numerical Linear Algebra with Applications*, **25**:e2167, 10 2018. https://doi.org/10.1002/nla.2167.

[15] S. Harizanov, S. Margenov, P. Marinov and Y. Vutov. Volume constrained 2-phase segmentation method utilizing a linear system solver based on the best uniform polynomial approximation of $x^{-1/2}$. *Journal of Computational and Applied Mathematics*, **310**:115–128, 1 2017. https://doi.org/10.1016/j.cam.2016.06.020.

[16] C. Hofreither. A unified view of some numerical methods for fractional diffusion. *Computers & Mathematics with Applications*, **80**(2):332–350, 7 2020. https://doi.org/10.1016/j.camwa.2019.07.025.

[17] C. Hofreither. An algorithm for best rational approximation based on barycentric rational interpolation. *Numerical Algorithms*, **88**(1):365–388, 9 2021. https://doi.org/10.1007/s11075-020-01042-0.

[18] W. Hundsdorfer and J. Verwer. *Numerical Solution of Time-Dependent Advection-Diffusion-Reaction Equations*. Springer, Berlin, Heidelberg, 2003. https://doi.org/10.1007/978-3-662-09017-6.

[19] F. Ivanauskas, V. Laurinavičius, M. Sapagovas and A. Nečiporenko. Reaction–diffusion equation with nonlocal boundary condition subject to PID-controlled bioreactor. *Nonlinear Analysis: Modelling and Control*, **22**(2):261–272, 3 2017. https://doi.org/10.15388/NA.2017.2.8.

[20] A.A. Kilbas, H.M. Srivastava and J.J. Trujillo. *Theory and applications of fractional differential equations.* Elsevier, Amsterdam, 2006.

[21] H.G. Lee. A second-order operator splitting Fourier spectral method for fractional-in-space reaction–diffusion equations. *Journal of Computational and Applied Mathematics*, **333**:395–403, 5 2018. https://doi.org/10.1016/j.cam.2017.09.007.

[22] R. Metzler and J. Klafter. The restaurant at the end of the random walk: recent developments in the description of anomalous transport by fractional dynamics. *Journal of Physics A: Mathematical and General*, **37**(31):161–208, 2004. https://doi.org/10.1088/0305-4470/37/31/R01.

[23] Y. Nakatsukasa, O. Séte and L. N. Trefethen. The AAA algorithm for rational approximation. *SIAM Journal on Scientific Computing*, **40**(3):A1494–A1522, 1 2018. https://doi.org/10.1137/16M1106122.

[24] R.H. Nochetto, E. Otárola and A.J. Salgado. A PDE approach to space-time fractional parabolic problems. *SIAM Journal on Numerical Analysis*, **54**(2):848–873, 3 2016. https://doi.org/10.1137/14096308X.

[25] I. Podlubny. *Fractional differential equations, mathematics in science and engineering.* Academic Press, New York, 1999.

[26] P.N. Vabishchevich. Splitting schemes for non-stationary problems with a rational approximation for fractional powers of the operator. *Applied Numerical Mathematics*, **165**:414–430, 7 2021. https://doi.org/10.1016/j.apnum.2021.03.006.

[27] H. Zhang, X. Jiang, F. Zeng and G.E. Karniadakis. A stabilized semi-implicit Fourier spectral method for nonlinear space-fractional reaction-diffusion equations. *Journal of Computational Physics*, **405**:109141, 3 2020. https://doi.org/10.1016/j.jcp.2019.109141.